



## Magnetic and meniscus-effect control of catalytic rolled-up micromotors

Jin-Xing Li<sup>a</sup>, Bing-Rui Lu<sup>a</sup>, Zhenkui Shen<sup>a</sup>, Zhencheng Xu<sup>a</sup>, Hui Li<sup>a</sup>, Juanjuan Wen<sup>a</sup>, Zhidong Li<sup>a</sup>, Xin-Ping Qu<sup>a</sup>, Yi-fang Chen<sup>b,\*</sup>, Yongfeng Mei<sup>c,d,\*</sup>, Ran Liu<sup>a,\*</sup>

<sup>a</sup>State Key Lab of ASIC and System, Fudan University, Shanghai 200433, China

<sup>b</sup>MNTC, Rutherford Appleton Laboratory, Chilton, Didcot, Oxfordshire, OX11 0QX, UK

<sup>c</sup>Department of Materials Science, Fudan University, Shanghai 200433, China

<sup>d</sup>Institute for Integrative Nanosciences, IFW Dresden, Helmholtzstr. 20, 01069, Dresden, Germany

### ARTICLE INFO

#### Article history:

Available online 28 January 2011

#### Keywords:

Catalytic motor  
Microtubes  
Motion control  
Rolled-up nanotech  
Meniscus-effect

### ABSTRACT

Rolled-up catalytic micromotors with tubular structures are fabricated by rolling up strained Pt/Co/Ti metallic nanomembranes through selectively etching of the sacrificial lift off resist (LOR). The rolled-up micromotors present distinct motion behaviors in an organic/aqueous mixture fuel compared to those in a pure aqueous fuel. These self-propelled micromotors can move in pure aqueous fuel with a speed up to several millimeters per second. However, when placed into an organic/aqueous mixture fuel, the micromotors walk on the liquid surface. An intermediate Co layer facilitates a magnetically guided motion of these microtubular motors. The motion at the air–liquid interface can be regulated and suspended by the meniscus-climbing effect. Such meniscus-navigated motion represents a novel approach for regulation of micromotors at the air–liquid interface and opens the door to new and exciting operations of these micro-scale machines.

© 2011 Elsevier B.V. All rights reserved.

### 1. Introduction

Fabrication and navigation of nanomotor to power nanomachines and nanofactories is one of the most active and challenging research areas in nanotechnology today [1]. During the past several years, researchers have made and developed the first generation of catalytic motors on the micro-/nanoscale [2–4]. By deriving energy from locally supplied fuels, these catalytic nanomotors hold autonomous non-Brownian movement to perform various tasks [5,6]. Despite enormous progresses have been achieved in motion control at the nanoscale [7], precise navigation of nanomotors is extremely challenging because of the combined problem of Brownian motion and low Reynolds numbers [8].

In this work, we present magnetic and meniscus-effect motion control of catalytic micromotors. The catalytic micromotors, which are fabricated by rolled-up nanotechnology [9], can move in the liquid or walk on the liquid surface when placed in different fuels. An intermediate Co layer can magnetically guide the motions of these microtubular motors. Furthermore, the motion on the liquid

surface can be regulated and suspended because of the attracting capillary force induced by the meniscus-climbing effect. Diverse moving patterns are presented when our micromotors are attracted by different capillary forces. These magnetically guided and meniscus-navigated motors show potential capabilities in diverse applications e.g. micro-scale manipulation, fabrication and assembly of micro-systems.

### 2. Experiment, results and discussion

Fig. 1 schematically presents the process flow to fabricate tubular micromotors. The lift off resist (LOR) delivered by the Micro-Chem Ltd., which is based on polymethylglutarimide (PMGI), was used as the sacrificial resist layer because its dissolvability in alkali chemicals and inertia in most organic solvents facilitate patterning the upper layers through photolithography and lift-off process [10]. On a Si substrate, the LOR was initially spin-coated and then pre-baked at 180 °C for 20 min. A photoresist layer (RFJ-220) was then lithographically patterned on the LOR layer. Strained Pt/Co/Ti (10/20/20 nm in thickness) metal films were deposited at 100 °C by physical vapor deposition (PVD) at a pressure of  $5 \times 10^{-5}$  Pa. After a lift-off process, metal films with square patterns were left on the LOR layer. The LOR layer was then selectively dissolved by a diluted alkali KOH solution, allowing the release of the deposited multiple metal layers. As a result, the planar multiple metal layers rolled up in a tubular-scroll. The tube diameter can be tuned by changing the thickness of the metal layers and strain [11],

\* Corresponding authors. Addresses: School of Microelectronics, Fudan University, 220, Handan Road, Shanghai, China. Tel.: +86 215 5664548; fax: +86 21 55664548 (R. Liu). Department of Materials Science, Fudan University, 220, Handan Road, Shanghai, China. Tel.: +86 21 65643615; fax: +86 21 65643615 (Y. Mei); Nanoscience & Nanotechnology Micro and Nanotechnology Centre. Tel.: +44 (0)1235 5159; mobile: 07788153503; fax: +44 (0)1235 6283 (Y. Chen).

E-mail addresses: [y.chen@rl.ac.uk](mailto:y.chen@rl.ac.uk) (Y.-f. Chen), [yfm@fudan.edu.cn](mailto:yfm@fudan.edu.cn) (Y. Mei), [rliu@fudan.edu.cn](mailto:rliu@fudan.edu.cn) (R. Liu).

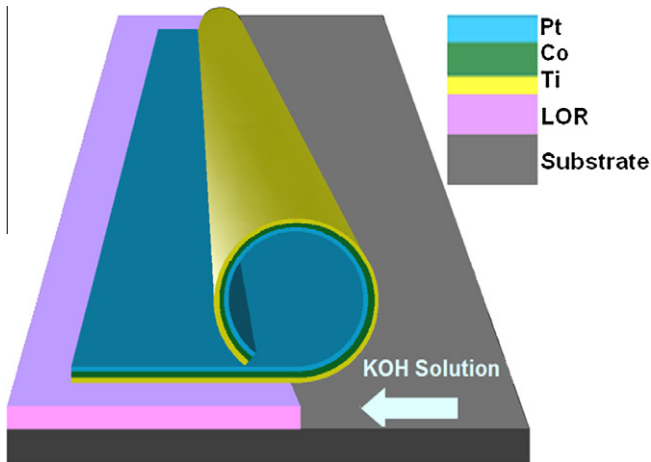


Fig. 1. Schematic diagram of the fabrication process for catalytic microtubular motors consisting of Pt/Co/Ti multilayers.

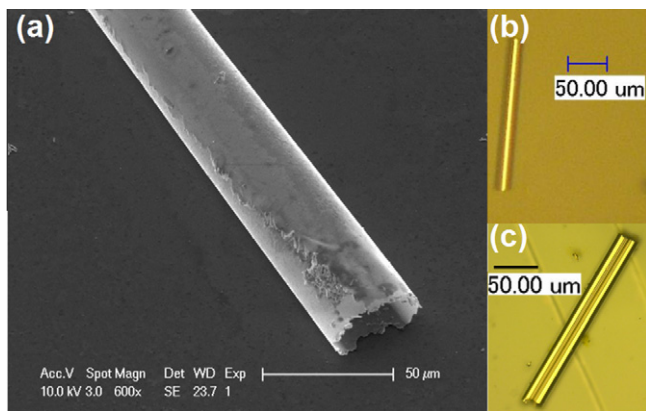


Fig. 2. (a) An SEM image of a rolled-up Pt/Co/Ti microtube. (b) Optical images of a rolled-up Pt/Co/Ti microtube and (c) a dual tube which can work as a dual-jet engine.

while the length can be controlled by predefining lithography patterns. Fig. 2a shows a scanning electron microscopy (SEM) image of a fabricated microtube with 35 μm in diameter and 200 μm in length. Fig. 2b displays an optical image of a rolled-up multimetallic microtube and Fig. 2c is an optical image of a dual-engine motor consisting of two parallel tubes rolling from opposite sides. Such dual-tube engine could offer more functions for the motion control of the motors.

The rolled-up micromotors present distinct motion behaviors in an organic/aqueous mixture fuel compared to those in a pure aqueous fuel. Fig. 3a displays time-dependent images for the autonomous movement of a microtubular motor in a 5% H<sub>2</sub>O<sub>2</sub> solution. A tail of micro oxygen bubbles (diameter: ~10 μm) catalytically generated on the inner Pt surface and released from the rear of the microtube, propels the motor forward at a speed of ~200 μm/s, corresponding to four body lengths per second. A higher speed can be obtained by a higher H<sub>2</sub>O<sub>2</sub> concentration. The dual-tube micromotors can present spiral and circular trajectories because of the different bubble ejection frequency of the two tubes caused by the shape asymmetry. Different from movement under the water surface in the pure aqueous fuel, the rolled-up microtubes can reside at the air-liquid interface when placed into a v/v 2:1 acetone/H<sub>2</sub>O solution. The catalytic micromotors in the organic/aqueous fuel, propelled by accumulated gas bubbles, can walk at a speed of up to ~10 body lengths per second on the liquid

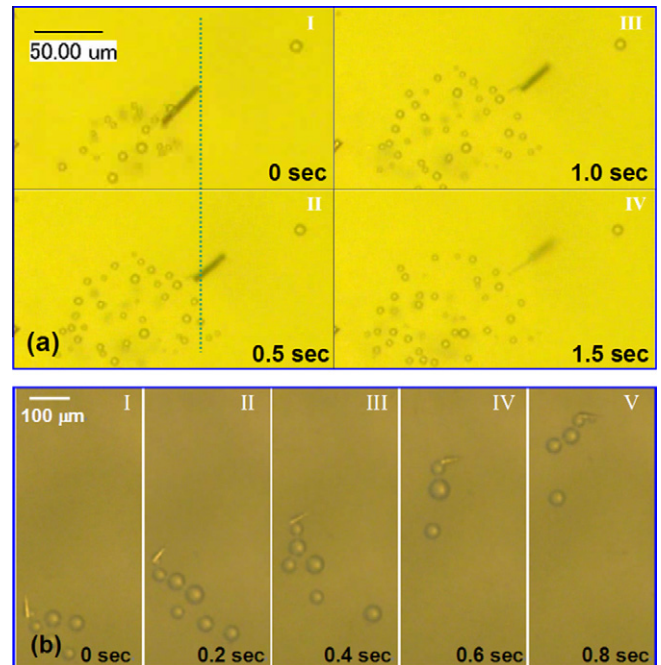


Fig. 3. (a) Timelapse images for the microtubular motor in a 5% H<sub>2</sub>O<sub>2</sub> solution at various time. (b) Magnetically-controlled movement of a microtube at the air-liquid interface in a v/v 2:1 acetone/H<sub>2</sub>O solution.

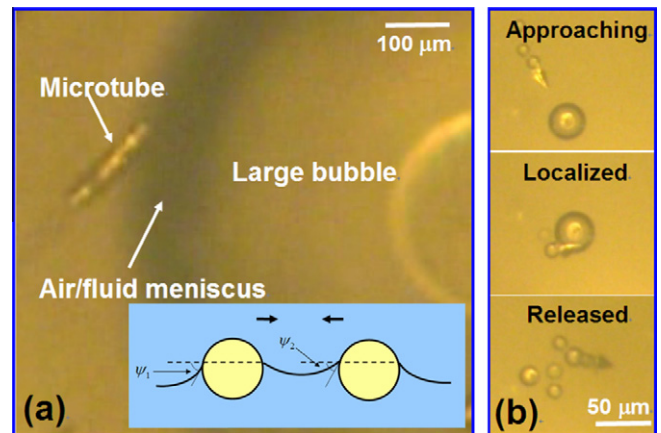
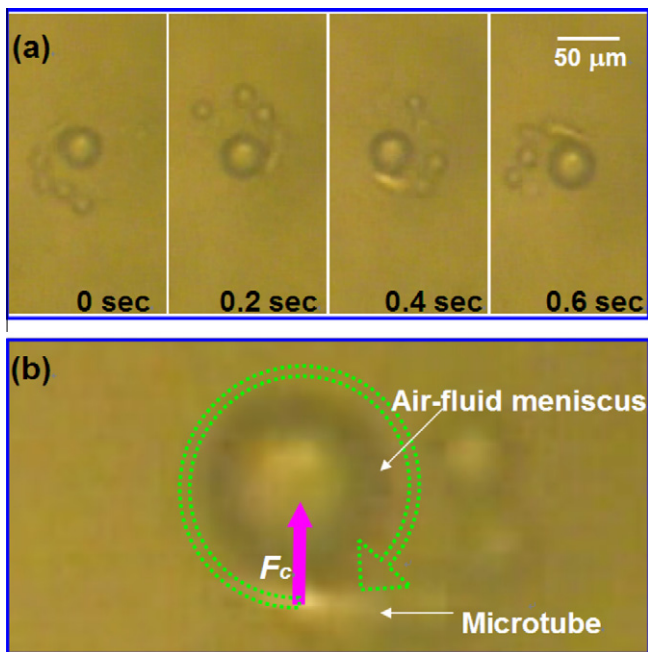


Fig. 4. (a) A moving microtube was anchored by the meniscus-effect at the border of a large bubble. Inset is schematic illustration of the capillary interaction of two small floating objects. (b) An off/on modulation of the micromotor base on meniscus-effect technique.

surface. This locomotion fashions are similar to the strider behavior of some water-walking insects which propel themselves at the water surface [12]. In previous work, it is considered that the microtubes at the air-liquid interface are lifted by buoyancy of oxygen bubbles in liquid [13]. However, the buoyancy in our organic/aqueous mixture fuel is even smaller than that in the aqueous fuel due to a lower density. This means that our microtubes which can reside on the liquid surface are exclusively supported by surface tension rather than the buoyancy. While using the catalytic motors to complete different tasks or move various cargos requires precise control of the autonomous moving direction, an intermediate Co layer was thus introduced to facilitate a magnetically guided motion of these microtubular motors. Fig. 3b displays the time-dependent images during the magnetically guided movement of the microtube on the liquid surface. Due to the presence of



**Fig. 5.** (a) Circular movement of a microtube when attached to a micro-object at the air–liquid interface. (b) Schematic illustration of the meniscus-climbing rotation initiated by attracting capillary force.

Co layer, the moving direction of catalytic micromotor can be changed longitudinally. However, axial velocity values are essentially unaltered by the presence of a magnetic field, because magnetic field only serves to orient the micromotors and it is the catalytic decomposition of hydrogen peroxide that serves to drive these tubes in solution.

We demonstrate that the existed lateral capillary force between small floating objects, an effect responsible for the meniscus-climbing behavior of certain types of water-walking insects [12], is promising and intriguing in controlling the motion of our micromotors. As illustrated in Fig. 4a, the moving microtube was anchored by the meniscus-effect at the border of a large floating bubble. A two-sphere model was used to illustrate the capillary interaction between a microtube and a floating object, as sketched in the inset of Fig. 4a. The rise of capillary forces, which can lead to the attraction of the two spheres, was given by the deformation of liquid–liquid interfaces due to two floating spheres. Kralchevsky et al. have provided the following asymptotic expression for calculating the lateral capillary force between two microspheres with radii of  $R_1$  and  $R_2$  when the center-to-center distance  $L$  is much smaller than the critical capillary length in certain liquid:

$$F_c = 2\pi\gamma r_1 \sin\psi_1 r_2 \sin\psi_2 / L [14],$$

where  $\gamma$  is the liquid–fluid interfacial tension,  $r_1$  and  $r_2$  are the radius of the two contact lines,  $\psi_1$  and  $\psi_2$  are the meniscus slope angles at the two contact lines. The attracting force between the object and the microtube can be tuned by the object radius which determines the radius of contact line. Thus we deduce that floating objects (e.g. bubbles) with various dimensions can serve to change the moving direction and regulate the speed of the micromotor.

As tuning off the motors by reducing the speed gradually is the most challenging because navigation principles used in the macro-scale world are not applicable to micro-scale propulsion [8], the interaction at the meniscus offers a telling way to constrain the activity of microtubes. Fig. 4b displays selected video images of

an off/on modulation of the micromotor base on meniscus-effect technique: a moving micromotor with a moving speed of  $\sim 50 \mu\text{m/s}$ , was slowed down and localized by a floating micro-object (here gas bubble) and released after the removing of the object. It is anticipative the micromotors can self-assemble into various patterns and systems by the meniscus-climbing technique.

In Fig. 5a, a high-speed moving catalytic microtube, which was attached to a round-shape bubble by the meniscus-induced capillary force, swam around the bubble with a rotational speed of  $\sim 15$  rad per second with a radius of  $20 \mu\text{m}$ . This circular motion of the catalytic microtube is interpreted in Fig. 5b. Catalytic microtube's moving direction is tuned by the capillary force  $F_c$ , which acts as a centripetal force on the microtube and then the tube holds the circular motion. However, as the capillary force increases with the radius of the floating object [14], a comparatively larger capillary force induced by a much bigger floating object will stop the moving of the motor due to corresponding larger resistance, just as the anchored micromotor illustrated in Fig. 4a. We also found that capillary interaction between the microtube and the micro-object is relevant to the size and the initial velocity of the microtube, thus various movement patterns can be achieved via tuning the size of microtubes and/or adjusting the concentration of  $\text{H}_2\text{O}_2$ .

### 3. Conclusion

In conclusion, we have demonstrated magnetic and meniscus-control of catalytic micromotors which are fabricated by rolling up strained Pt/Co/Ti metallic nanomembranes. Water-walking behaviors of the microtubes are investigated in organic/aqueous mixture fuel. The motion of the micromotors can be controlled by magnetic-field and the meniscus-induced capillary force. Diverse motion behaviors indicate that the micromotors can be elaborately assembled and anchored at the air–liquid interface. These new performances of the micromotors offer opportunities for novel bio-inspired devices and self-assembly micro-systems.

### Acknowledgements

The authors would like to thank financial support from Shanghai Municipal of Science and Technology (08QH14002), National Basic Research Program of China (2006CB302703), and the Seed Funds for Key Science and Technology Innovation Projects of MOE (708020). This work is also supported by the “985” Micro/Nanoelectronics Science and Technology Platform.

### References

- [1] T.E. Mallouk, A. Sen, *Sci. Am.* 300 (2009) 72–77.
- [2] W.F. Paxton, K.C. Kistler, C.C. Olmeda, A. Sen, S.K.S. Angelo, Y. Cao, T.E. Mallouk, P.E. Lammert, V.H. Crespi, *J. Am. Chem. Soc.* 126 (2004) 13424–13431.
- [3] A.A. Solovev, Y.F. Mei, E.B. Urena, G.S. Huang, O.G. Schmidt, *Small* 14 (2009) 1688–1692.
- [4] S. Fournier-Bidoz, A.C. Arsenault, I. Manners, G.A. Ozin, *Chem. Comm.* 441 (2005) 441–443.
- [5] S. Sundararajan, P.E. Lammert, A.W. Zudans, V.H. Crespi, A. Sen, *Nano Lett.* 8 (2008) 1271–1276.
- [6] J. Burdick, R. Laocharoensuk, P.M. Wheat, J.D. Posner, J. Wang, *J. Am. Chem. Soc.* 130 (2008) 8164–8165.
- [7] J. Wang, K.M. Manesh, *Small* 3 (2010) 338–345.
- [8] E.M. Purcell, *Am. J. Phys.* 45 (1977) 3–11.
- [9] O.G. Schmidt, K. Eberl, *Nature* 410 (2001) 168.
- [10] Y. Chen, K. Peng, *Microelec. Eng.* 73–74 (2004) 278–281.
- [11] Y.F. Mei, G.S. Huang, A.A. Solovev, E.B. Urena, I. Monch, F. Ding, T. Reindl, R.K.Y. Fu, P.K. Chu, O.G. Schmidt, *Adv. Mater.* 20 (2008) 4085–4090.
- [12] D.L. Hu, J.W.M. Bush, *Nature* 437 (2005) 733–736.
- [13] A.A. Solovev, Y. Mei, O.G. Schmidt, *Adv. Mater.* doi:10.1002/adma.201001468.
- [14] P.A. Kralchevsky, K. Nagayama, *Adv. Colloid Interface Sci.* 85 (2000) 145–192.